Hindawi
Geofluids
Volume 2023, Article ID 4208655, 12 pages
https://doi.org/10.1155/2023/4208655

Research Article

Experimental Study on Residual and Dissolution of DNAPL in Transparent Fracture

Junyu Wu[1,2] **Shu Zhu**[1,2] **Zhende Zhu**[1,2] **Bin Lu**[3] **and Luxiang Wang**[1,2]

[1]*Key Laboratory of Ministry of Education for Geomechanics and Embankment Engineering, Hohai University, Nanjing 210098, China*
[2]*Jiangsu Research Center for Geotechnical Engineering Technology, Hohai University, Nanjing 210098, China*
[3]*State Key Laboratory of Hydrology-Water Resources and Hydraulic Engineering, Nanjing Hydraulic Research Institute, Nanjing 210029, China*

Correspondence should be addressed to Shu Zhu; 20210940@hhu.edu.cn

Received 14 October 2022; Revised 26 November 2022; Accepted 10 December 2022; Published 11 January 2023

Academic Editor: Hetang Wang

Dense nonaqueous phase liquid (DNAPL) is one of the main pollution sources of the underground environment. After DNAPL enters the underground environment, the migration and diffusion process has experienced a variety of media, resulting in large-scale and long-term pollution. To better understand the residual and dissolution process of DNAPL in fractures, the visual experiment of DNAPL residual and dissolution in the fracture was carried out using the transparent fracture model made of glass material, and the changes of DNAPL migration morphology and residual distribution in the crack were obtained. The results showed that the migration front of DNAPL in the fracture was finger shaped in the process of displacement of water phase by DNAPL phase, which was consistent with the state in porous media. When the process of water phase displacing DNAPL phase was over, discrete and aggregated DNAPL droplets remained in the fracture. The residual DNAPL was mainly concentrated in the area ranged from 0.3 mm to 0.8 mm. The dissolution rate of DNAPL in the fracture changed from fast to slow, and there was an obvious tailing period. The increased velocity of water phase flow significantly shortened the time of dissolution process. The DNAPL with hydrolysis reaction accounted for only 0.86% on average in the dissolution process. The findings of this study are helpful to the remediation of the underground environment.

1. Introduction

Groundwater, as one of the important sources of human water, is being increasingly polluted [1–3]. Among all these pollution sources, organic pollutants pose great threat to human health and natural environment. Dense nonaqueous phase liquid (DNAPL) is one of the sources of organic pollutants in groundwater [4–6]. Due to its high viscosity, low solubility, and degradability [7], DNAPL is the focus of prevention and protection of underground environmental pollution [8–10]. As is shown in Figure 1 [11], the migration and diffusion path of DNAPL in the underground environment is complex. It is important to study the migration of DNAPL in the underground environment for the remediation of pollutants.

In the early stage, studies on the pollution problem of DNAPL were mainly conducted by one-dimensional and two-dimensional laboratory setup. Through constructing a heterogenous sand-pack cell, Kueper and Frind [12] qualitatively studied the influence of heterogeneous porous media on the displacement of water by DNAPL and verified the critical role of capillary characteristics in the migration

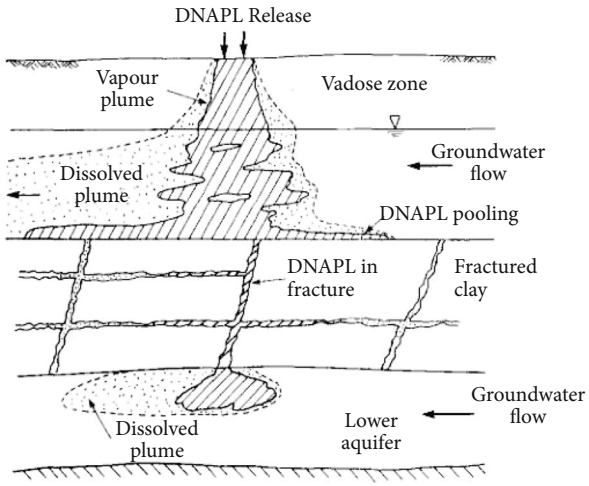

Figure 1: Migration and diffusion process of DNAPL in underground environment [11].

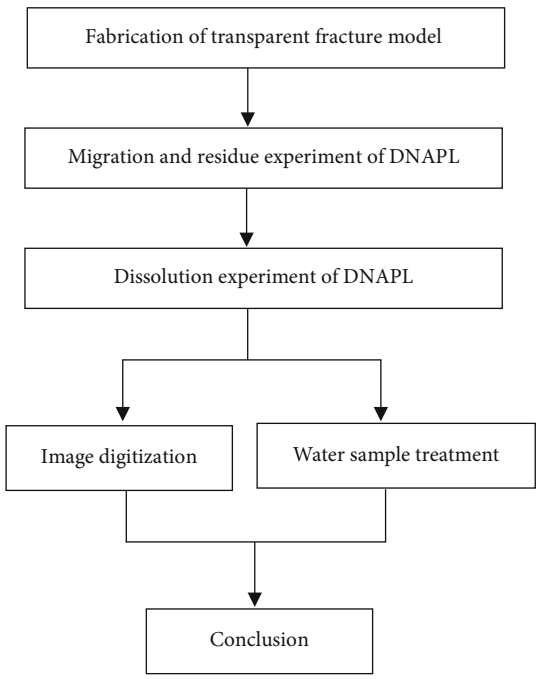

Figure 2: Flowchart of the experiment steps.

process. Zhang and Smith [13] carried out a two-dimensional visualization experiment of DNAPL penetrating into saturated porous media and described and analyzed the mechanism of DNAPL-fingering process. The results showed that the fingering process may be divided into the finger initiation stage and the finger elongation stage. Gao et al. [14] selected PCE as the substitute containment and performed two-dimensioned sandbox experiments. They found that the increased velocity promoted both lateral and vertical migration of DNAPL, leading to an inclined percolation path.

In addition to model experiments, mathematical models and numerical simulation methods were also used to study DNAPL [15–17]. According to the law of conservation of mass, Abriola and Pinder [18] established a one-dimensional implicit numerical model of multiphase migration equations of organic matter in the ground. The model comprehensively considered the three-phase relative permeability, distribution coefficient, mixture density and viscosity, and other parameters. Abriola and Pinder used this model to simulate the infiltration of hydrocarbon mixture in soil column, the migration of organic matter in gas and water phases, and the migration of pollutant plume. By using TMVOC and PetraSim to conduct multiphase modeling, Erning et al. [19] found that high-groundwater flow velocities would change the geometry, the architecture, and mainly the position of a TCE source zone significantly. As a result, this led to a direct influence on the dissolution behaviour, the mass transfer rates, and the longevity of DNAPL. All these studies mainly focused on the problem of DNAPL contamination in porous media.

Compared with studies on porous media, studies on DNAPL pollution in fractured media [20, 21] were relatively less. Weerakone and Wong [22] simulated the process of DNAPL water two-phase flow in fractures using the intrusion seepage method and studied the influence of fracture characteristics on DNAPL migration process. Zhu et al. carried out a dissolution experiment of DNAPL in a three-dimensional fracture system to evaluate the dissolution kinetics of tetrachloroethylene (PCE) DNAPL under residual saturation under environmental groundwater conditions. In recent years, with the wide application of transparent rock-like materials in various experiments [23], DNAPL visualization experiments in fractured media have also been realized [24]. Chen et al. [25] made use of resin materials to copy the rough cracks and carried out experiments, obtained the phase diagram of displacement mode of DNAPL in a rough crack, conducted qualitative and quantitative analyses on the DNAPL invasion morphology, and determined the boundaries of capillary finger, viscous finger, dense displacement, and cross areas. At the present stage, the visualization experiment of pollutants using transparent fractures is mainly focused on the short-term migration and displacement process. To our knowledge, few people use transparent fractures to carry out visual experiments to study the dissolution behavior of DNAPL in fractured medium.

In the actual process, DNAPL exists in fractured medium for a long time due to its low solubility, causing long-term pollution of the underground environment. Therefore, in this paper, DNAPL residual and dissolution experiment was carried out using a transparent replica fracture. The geometric distribution characteristics and residual distribution of DNAPL during short-term migration process and the residual distribution changes of DNAPL during long-term dissolution process were analyzed. The changes of DNAPL residues under different water phase flow rates were compared. In the first step of this experiment, we made a transparent fracture model with shale as the prototype. Then, we used transparent model to carry out DNAPL migration experiment in fractures and obtained the residual distribution. Finally, the dissolution test was carried out on the basis of the residual distribution of DNAPL. The flowchart of the experiment steps is shown in Figure 2. This experiment improves our understanding of the residual distribution and dissolution of DNAPL in fractured medium

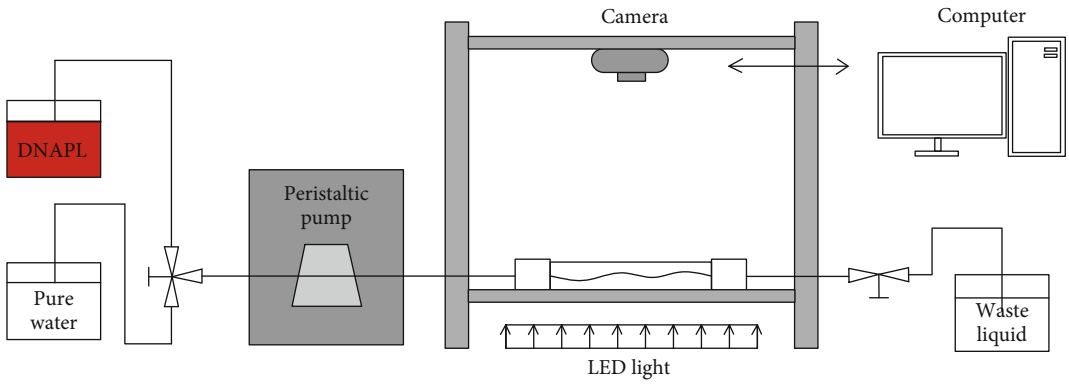

Figure 3: Schematic diagram of experimental apparatus.

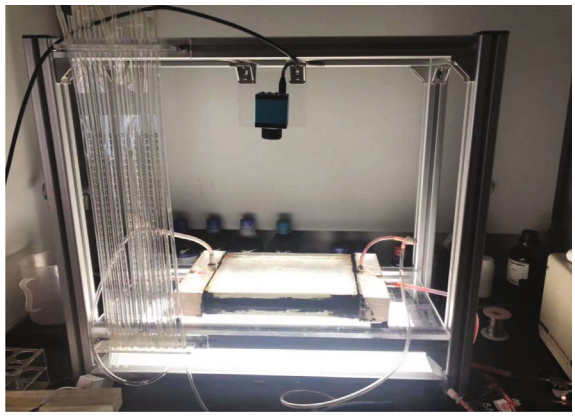

Figure 4: Main part of experimental apparatus.

and provides a certain reference for the remediation of DNAPL in the underground environment.

2. DNAPL Residual and Dissolution Experiments in the Fracture Model

2.1. Experimental Apparatus. The experimental apparatus was composed of a transparent fracture, image acquisition system (including high-definition camera and computer), and replenishment system. The transparent crack was placed on the transparent glass plate. A high-definition camera connected to the computer was set on the top, and an LED light was set under the transparent glass plate, which made the brightness of photos collected by the camera uniform and stable. The two sides of the fracture model were, respectively, connected with the replenishment system and the waste liquid tank. The replenishment system was composed of a peristaltic pump and containers containing pure water and DNAPL, respectively. The overall schematic diagram of the experimental apparatus is shown in Figure 3. Figure 4 is a photo of the main part of the experimental apparatus taken during the experiment.

In order to directly observe the distribution of DNAPL in the fracture, a fracture model was made with transparent glass material using shale fracture as the prototype. The use of glass material can make the replicated fracture have a surface wettability similar to that of the rock surface. This is an effective method for studying two-phase flow in fractures [26]. The fracture was obtained by splitting a shale rock, and the plane size was 270 mm × 200 mm. The aperture distribution is shown in Figure 5.

In addition, spectrophotometer, laboratory grade ultrapure water device, beaker, and other common test instruments are also used in this test.

2.2. Experimental Materials and Methods. PCE (tetrachloroethylene), as a typical chlorinated organic compound, is colorless and has a pungent odor, which is one of the common DNAPL pollutants. In this experiment, we selected PCE as the representative pollutant of DNAPL. Physical and chemical properties of PCE are shown in Table 1.

Before the experiment, some preparations need to be completed. First of all, we need to dye the PCE fluid. Since the PCE liquid was transparent, we could not distinguish PCE liquid from water directly. In order to distinguish water and PCE significantly, Sudan III was used to dye PCE to make it red. In addition, the gas existing in the fracture should be discharged, so as to eliminate the interference of gas to the experimental process. Here, we chose to continuously inject distilled water into the fracture. This process continued until no bubbles were observed in the fracture model.

The experiment was divided into two parts. The first part was a short-term migration process. In this process, the migration of DNAPL in the fracture was observed and the initial residual distribution of DNAPL was obtained. This process lasted only a few minutes. After observing that the fracture was saturated and free of bubbles, we adjusted the computer program and set the photographing interval of the HD camera to 1 second. The PCE was continuously injected into the fracture. The whole process of PCE migration was observed and recorded. After that, pure water was injected into the fracture to flush the PCE until the residual distribution of PCE was stable.

The second part of the experiment was a long-term dissolution process, in which the dissolution of DNAPL remaining in the fracture was observed. This process lasted for several days. During this process, the time interval of taking the picture was 1 day. Pure water was continuously injected into the fracture and the change of residual PCE

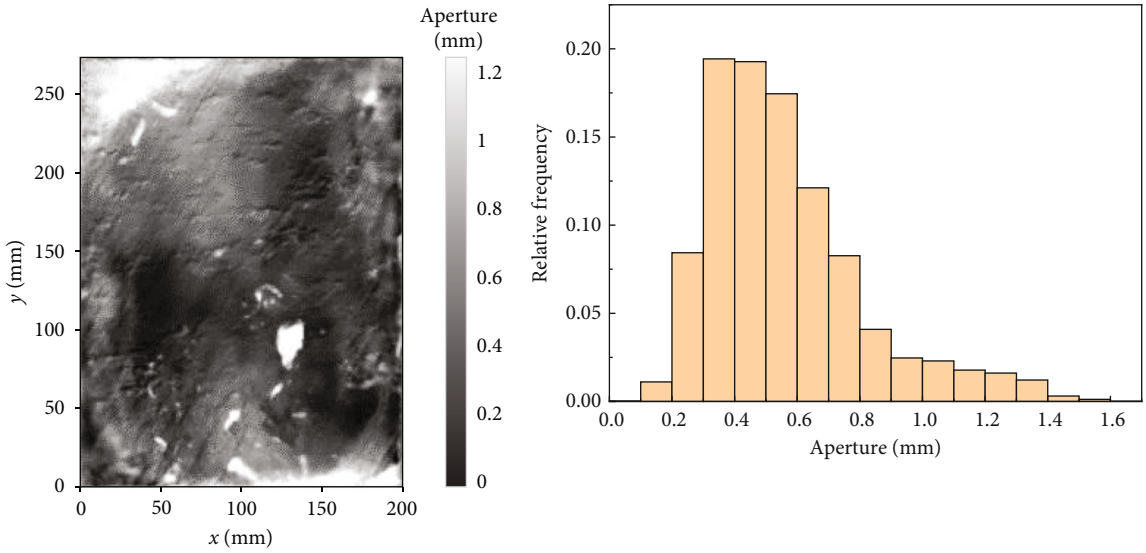

Figure 5: The aperture distribution of the fracture.

Table 1: Characteristics of DNAPL.

DNAPL	Molecular formula	Density (g/cm^3)	Viscosity coefficient
PCE	C_2Cl_4	1.63	0.84

Table 2: Experimental design.

Group	Residual quantity (g)	Initial area (mm^2)	t (d)	Q (mL/s)
R1	44.0	7658.52	62	0.06
R2	33.2	5600.33	20	0.14
R3	31.7	5443.20	12	0.28

distribution was observed and recorded. The details of the dissolution experiment are given in Table 2.

The analysis of this experiment was based on the collected photos and water samples. In order to extract efficient information from the photos and obtain specific data, a series of processing were carried out on the photos. The first step was to use the image-processing software to batch process the photos taken by the camera, cut out the part of the fracture model, and convert it into a grayscale image. Then, by selecting an appropriate threshold, the gray image was converted into a binary image. After that, the binary distribution map of PCE in the fracture was obtained. Finally, a series of functions in the processing software were used to calculate the area and other parameters of PCE. The photo-processing procedure is shown in Figure 6.

In addition to image processing, the collected water samples were also analyzed. The analysis of water samples was divided into two parts, one was to determine the concentration of PCE in the water samples by gas chromatography and the other was to determine the concentration of chloride ions in the water samples by spectrophotometry. The dissolution process of PCE in fractures is relatively complex, and hydrolysis reaction may occur in addition to water dissolution. Some PCE will undergo hydrolysis reaction in contact with water phase to generate trichloroacetic acid and hydrogen chloride. In this experiment, the spectrophotometer method was used to measure the concentration of trace chloride ions in the water sample. Chloride ions and silver ions will react to produce silver chloride precipitation. Due to the instability of silver chloride precipitation, the results of direct application in spectrophotometric determination of chloride concentration are often not ideal. The silver chloride precipitation can stably exist in the gelatin ethanol aqueous solution. As a result, the concentration of chloride ion can be determined by spectrophotometry in the gelatin ethanol aqueous solution system.

When the concentration of chloride ion was determined by spectrophotometry, it was necessary to draw a standard curve first. Before drawing the standard curve, it is necessary to determine the selection of each parameter in the spectrophotometry. The parameter in the spectrophotometry was the optimal wavelength of the spectrometer, the amount of nitric acid, the amount of silver nitrate, and the amount of gelatin ethanol aqueous solution. After a large number of experiments, it was determined that the light wavelength of the spectrophotometer is 310 mm, the amount of nitric acid required in one single calibration is 2.5 mL, the amount of silver nitrate is 1.5 mL, and the amount of gelatin ethanol aqueous solution is 2 mL.

Figure 7 shows the formula of standard curve

$$y = 0.8511x - 0.0125, \quad (1)$$

where x (mg/L) is the chloride ion concentration and y is the light absorption value. According to the standard curve, we

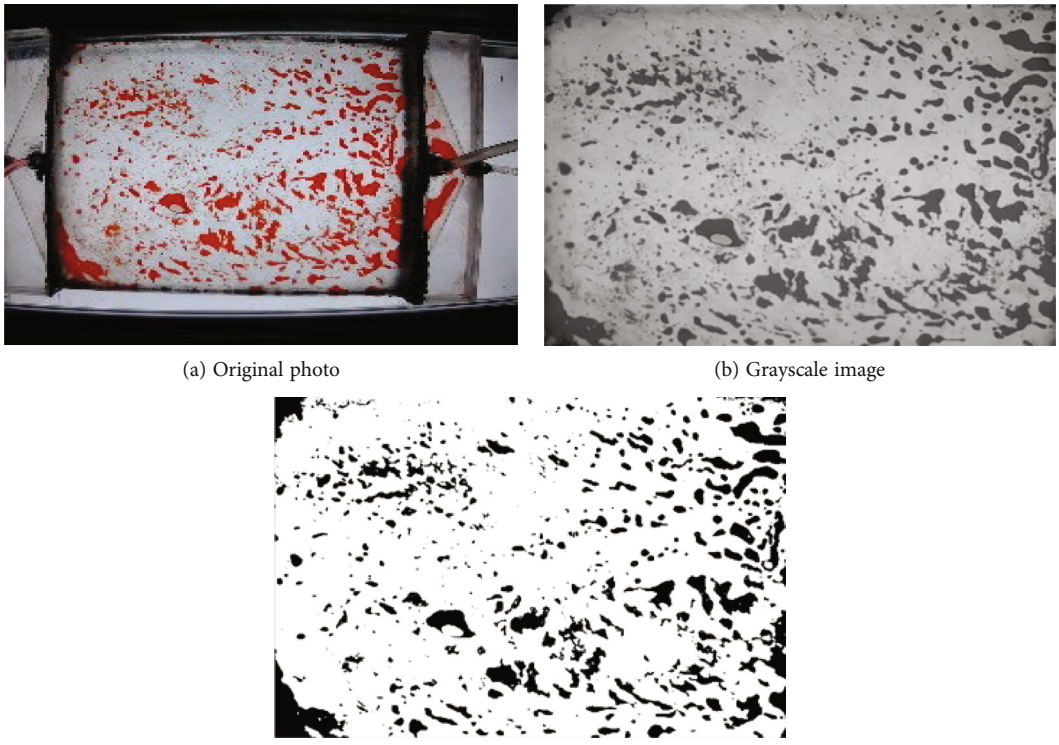

(a) Original photo

(b) Grayscale image

(c) Binary image

Figure 6: Photo-processing procedure.

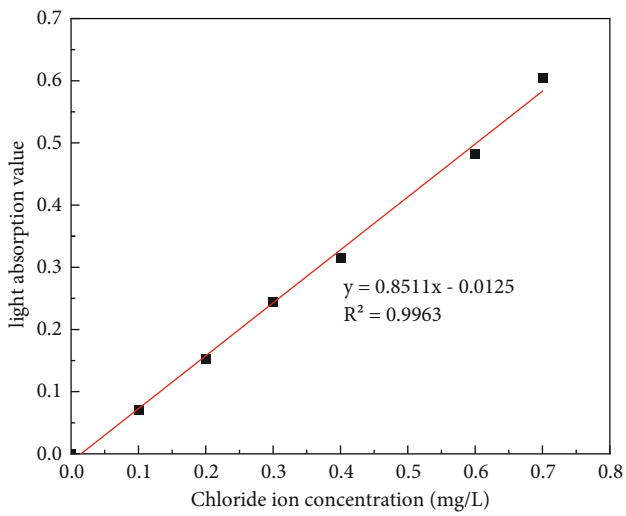

Figure 7: Parameters and standard curve of spectrophotometry.

can calculate the concentration of chloride ion in the solution by the measured absorbance value.

3. Experimental Results

3.1. DNAPL Migration Process. The migration process of PCE in the fracture model is shown in Figure 8. At the initial stage of migration experiment, PCE intruded into the saturated fracture. Since PCE was insoluble in water, two-phase flow was formed in the fracture, and DNAPL phase-displaced water phase migrated in the fracture model. When PCE started to enter the fracture, it migrated in both horizontal and vertical directions. In the initial few seconds, the vertical migration speed was significantly greater than the horizontal migration speed. After nearly 20 seconds, the migration path of PCE was mainly horizontal migration. After 30 seconds, PCE first broke through the whole fracture from the bottom to enter the tail joint of the model and flowed into the waste liquid pool. The front end of PCE fluid migration was finger shaped, which was similar to the migration morphology observed in porous media.

Due to the anisotropy of fracture media, the hydraulic conductivity of each area of the fracture was different, which lead to the uneven flow of water in fractured medium. The nonuniform flow of water made the dominant flow form at the concentration of water flow in fractured medium. Dominant flow was an important feature of fractured media, and the "advantage path" was the path through which the dominant flow passed. Similarly, PCE also had three "dominant paths" in the migration of the saturated fracture. As is shown in Figure 9, the "dominant path" below was relatively narrow, followed by the upper path, and the middle path was the widest. The PCE in the "advantage path" below took the first time to pass through the whole fracture, followed by the path in the middle, and finally the path above. After the PCE in the three "advantage paths" had passed, the vertical migration of PCE did not stop but was still growing slowly, and the total amount of PCE in the fracture was also growing slowly.

The change of total PCE area in the fracture is shown in Figure 10. Assuming that the total amount of PCE in the fracture is replaced by the area of PCE, it can be seen

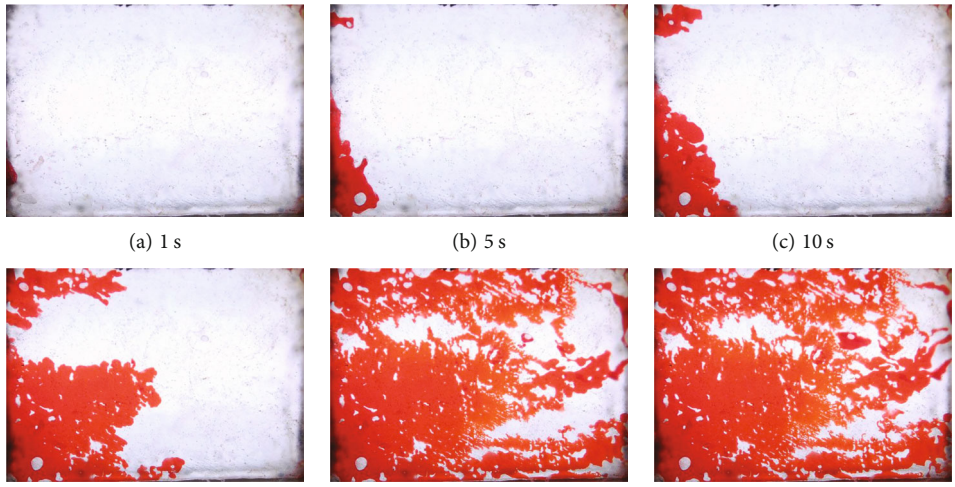

Figure 8: Migration process of PCE in the fracture model.

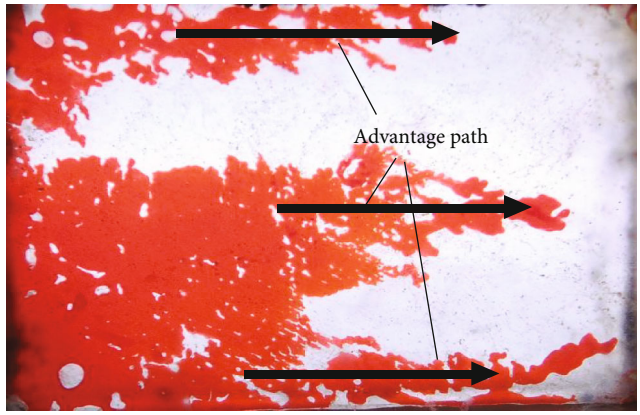

Figure 9: Advantage path in PCE migration.

from the PCE area change curve that the migration of PCE in the fracture can be divided into three stages. In the first stage, the total amount of PCE in the fracture increased linearly. All PCE in this stage existed in the fracture. Since the rate of PCE invading the fracture is constant, the total amount of PCE in the fracture was proportional to the time. At the beginning of the second stage, some PCE started to flow into the waste liquid pool, while the total amount of PCE in the fracture was still increasing significantly, and the increase rate gradually slowed down. In the third stage, the total amount of PCE in the fracture kept constant. The DNAPL phase and the water phase form a stable distribution, and all injected PCE flowed into the waste liquid pool.

3.2. DNAPL Residual Distribution. When the injection of PCE into the fracture model was stopped and pure water was injected instead, the two-phase rheology in the fracture became a process of water phase displacing DNAPL phase. At the initial stage, PCE was discharged from the fracture in a concentrated state, and most PCE was displaced by water flow and flowed into the waste liquid pool. At this stage, the total PCE in the fractures decreased rapidly. With the continuous injection of water flow, some discrete small droplets leave the fracture with the water flow. In this stage, a few PCE droplets were discharged with the water flow, and the total amount of PCE remaining in the fracture was slowly reduced. The rate of total PCE reduction was significantly slower. At the final stage, the residual PCE in the fracture was basically stable; the total amount of PCE was almost unchanged. Only a few liquid drops flowed to the waste liquid pool with the water flow. The final residual PCE in the fracture mainly existed in two states: discontinuous discrete droplets with small area (area B in Figure 11) and aggregated droplets with large area (area A in Figure 11). Comparing the residual status with the gap width distribution map, it can be found that discrete droplets were mainly concentrated in the area with smaller aperture, while aggregated droplets were mainly concentrated in the area with larger aperture. The final residual distribution of PCE in the fracture is shown in Figure 11.

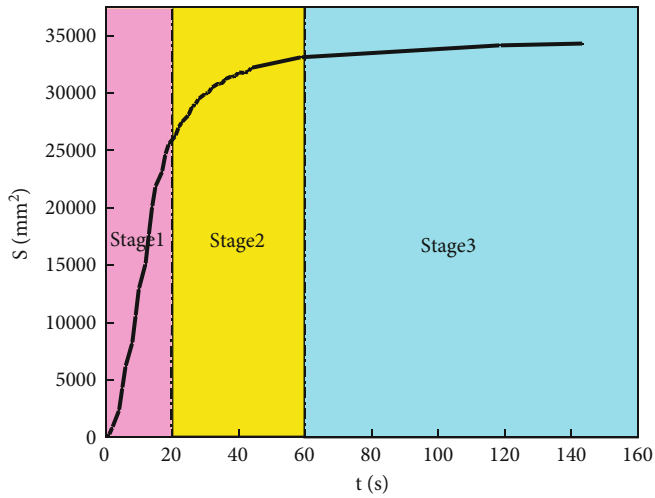

Figure 10: Area curve of PCE.

Figure 11: Residual distribution of PCE in fracture model.

The efficiency of displacing DNAPL phase by water phase is directly related to the hydraulic conditions of water phase [27]. The displacement fluid movement is described by Reynolds number, and the Reynolds number Re of the displacement fluid in a single fracture is

$$\mathrm{Re} = \frac{\rho Q}{\mu W}, \tag{2}$$

where ρ is the displacement fluid density, Q is the displacement flow, W is the aperture, and μ is the dynamic viscosity. The displacement efficiency is positively correlated with Reynolds number. When the aperture is small, the Reynolds number is large, and the displacement efficiency of the aqueous phase is low.

Since it was difficult for PCE to enter the interval with small aperture, there were fewer PCE in the interval with smaller aperture when the water phase had not started to displace the DNAPL phase. As a result, few PCE residues were distributed in the area with relatively small aperture. On the contrary, PCE was more distributed at the place with larger aperture. However, the hydraulic conditions at the place with larger aperture were better. The efficiency of aqueous phase displacement of PCE was higher, so the residual PCE was less in the section with larger aperture.

Figure 12 shows the distribution of the residual PCE in multiple flushing experiments. It was obtained by comparing the binary map of the residual distribution of PCE in the fracture with the aperture distribution. The large map is the histogram of the relative frequency of each aperture interval, and the small map is the cumulative curve of the aperture distribution. It can be seen from Figure 12 that the main residual distribution of PCE in multiple flushing experiments is consistent with the distribution of aperture. In these flushing experiments, the residual distribution of PCE was concentrated in the range of 0.3 to 0.8 mm, and the residual amount was relatively small when the aperture was less than 0.3 mm and more than 0.8 mm. These cumulative frequency curves of PCE distribution show a consistent trend. The cumulative frequency increased slowly in the range of 0 to 0.3 mm. In the range of 0.3 mm to 0.8 mm, the frequency increased rapidly.

3.3. DNAPL Dissolution Process. During the dissolution process, the dissolution rate of PCE in the fracture changed continuously. At the beginning of the dissolution process, the dissolution rate was fast, discrete droplets dissolve and disappeared, and aggregated PCE gradually shrank. Then, the dissolution rate was significantly slowed down, discrete droplets were basically dissolved completely, and the remaining PCE-aggregated drops were also much smaller than the initial stage. The remaining PCE was mainly distributed at the places with small aperture. This was caused by the nonuniform flow of water due to the nonuniformity of the fracture, which also led to the nonuniformity of PCE dissolution process in the fracture. Figure 13 shows the change process of PCE residual distribution in R1 experiment.

Figure 14 shows the comparison of PCE residual distribution and initial residual distribution on the 30th day of R1 experiment. It can be found from the comparison between

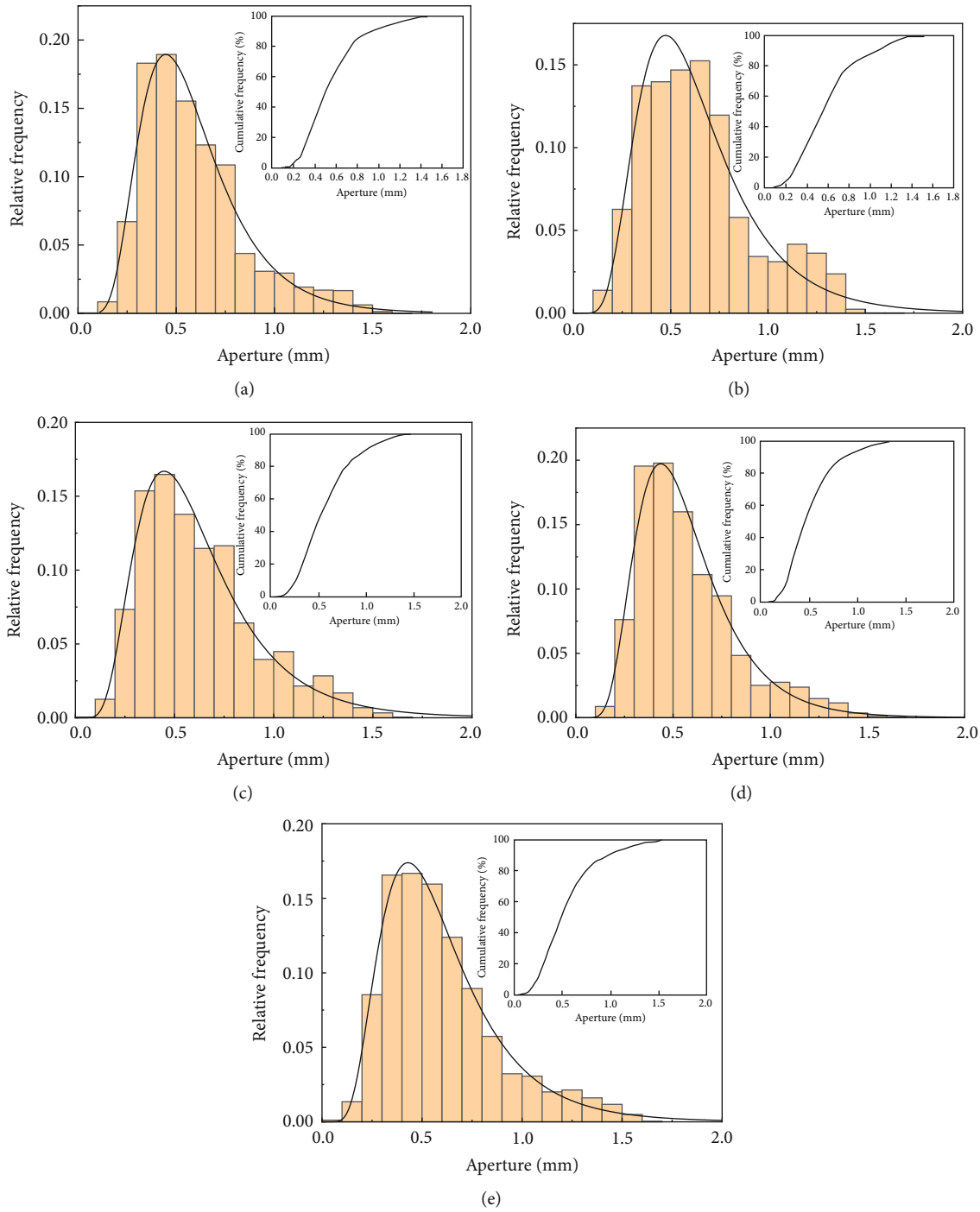

Figure 12: Statistics of aperture distribution of PCE residues.

areas A and B in Figure 14 that along the water flow direction, the PCE dissolution near the water inlet was relatively more than that near the water outlet. The changes in areas A and C reflect the dissolution of droplets with smaller discrete areas. The changes in area D show the dissolution of droplets with larger aggregated areas. These changes indicate that small discrete droplets were more easily dissolved than those larger aggregated droplets.

In experiments R1, R2, and R3, the velocity of water phase flow is 0.06 mL/s, 0.14 mL/s, and 0.28 mL/s, respectively (Figure 15). Although the initial quantities of PCE in three groups were different, it is found by comparison that the dissolution rate of PCE in the fracture increased significantly with the increase of the water phase flow rate. Compared with R1, the quantity of PCE in R2 decreased by 24.5%, but the time required for complete dissolution was only 32.3% of the time required in R1. The quantity of PCE in R3 was 28.0% less than that in R1, but the time required for complete dissolution was only 19.6%. By comparing the area change in three groups, the dissolution rate of PCE in experiments R1, R2, and R3

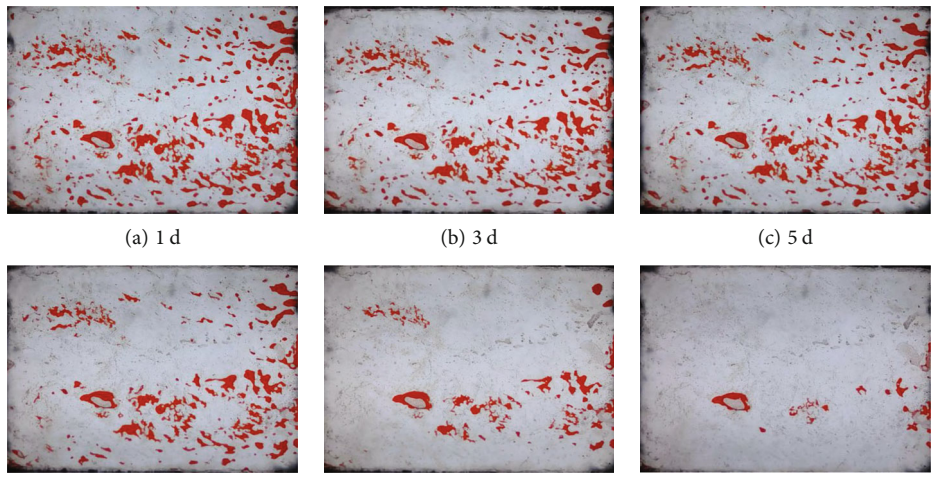

Figure 13: Dissolution process of PCE in the fracture model.

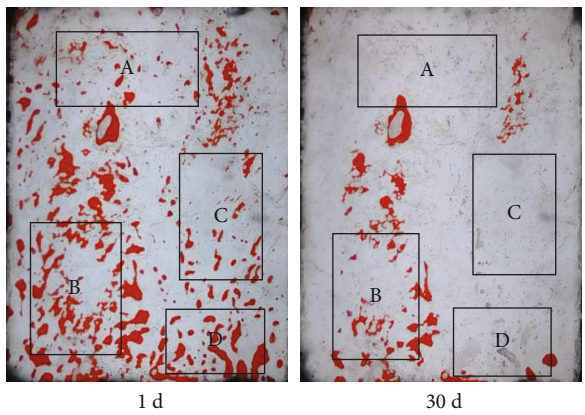

Figure 14: Comparison of PCE residue distribution.

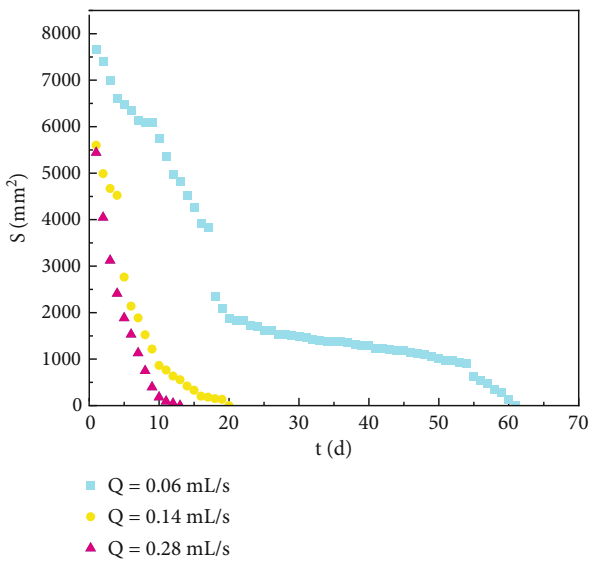

Figure 15: Dissolution process of PCE in the fracture model.

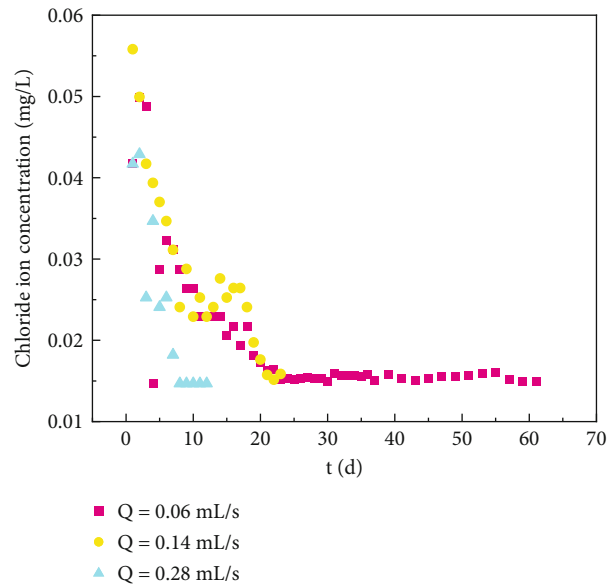

Figure 16: Scatter plot of chloride ion concentration change.

Table 3: Characteristics of DNAPL.

Group	PCE quantity (g)	PCE quantity of hydrolysis reaction (mg)
R1	44.0	23.98
R2	33.2	36.87
R3	31.7	32.31

showed a significant change from fast to slow, and there was a significant tailing phenomenon at the end of dissolution. However, with the increase of the velocity of water phase flow, the time of tailing was significantly shortened. Compared with the area change curve in R1, the curve of R2 is steeper and the rate

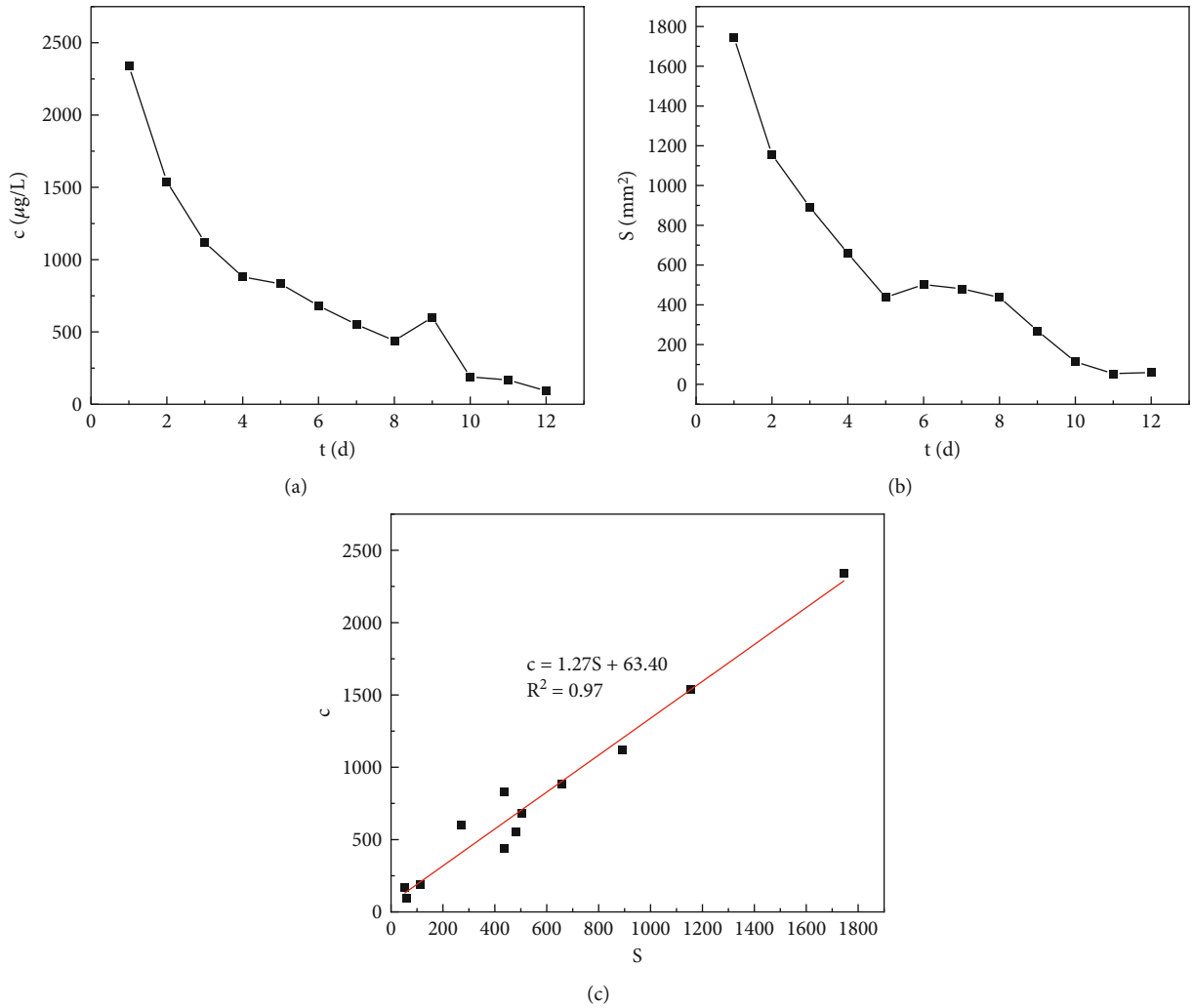

Figure 17: PCE concentration and area change.

of decline was faster, which indicated that the change of dissolution rate in R2 was greater. Similarly, the change of dissolution rate in R3 was faster than that in R2. These phenomena indicate that the dissolution rate of PCE in the fracture increased significantly with the increase of the water phase flow rate, and the rate of dissolution rate change also increased.

The dissolution process of DNAPL was affected by several actions, including water phase flow, dissolved DNAPL migration, interface mass transfer, and corresponding DNAPL water interface movement [28–31]. With the dissolution process, the interface area of DNAPL aqueous phase decreased continuously, which led to the slower dissolution rate of DNAPL. Therefore, the curve of DNAPL changes with time presented a downward trend. Therefore, the dissolution process of DNAPL was significantly accelerated with the increase of water flow rate.

In these three groups, the effluent was collected at an interval of 24 hours. The absorbance value of the solution was determined by spectrophotometry, and the concentration of chloride ion was calculated according to the standard curve. It can be seen from the chloride ion concentration distribution diagram (Figure 16) that the change trend of partial concentration of PCE hydrolysis reaction was consistent with that of PCE concentration. And there was also an obvious tailing period.

Assuming that the chloride ion concentration in the effluent water sample was the average value of the chloride ion concentration in the water of the day. On this basis, we estimated the mass of tetrachloroethylene in hydrolysis reaction, and the estimated results are shown in Table 3. The tetrachloroethylene in hydrolysis reaction only accounted for a small part of the residual tetrachloroethylene in the fracture, with an average of 0.86%. As the consumption of tetrachloroethylene in hydrolysis reaction was relatively low, the hydrolyzed part of tetrachloroethylene may not be considered in the dissolution process.

The transparent fracture made of glass material could help us directly observe the situation of DNAPL. However, the total volume of DNAPL in the fracture was difficult to measure directly. Here, we compare and analyze the change of PCE area in the transparent fracture and the concentration of PCE. The concentration of PCE in the effluent was determined by gas chromatography.

By comparing and analyzing the PCE concentration curve (Figure 17(a)) and PCE area change value curve (Figure 17(b)) in the effluent, we find that these two curves have similar trends and there is a linear relationship between them. The relationship between PCE concentration c and PCE area change value S is $c = 1.27S + 63.40$, and the goodness of fit is $R^2 = 0.97$. Therefore, it is a simple and reliable method to replace the total amount of PCE with the area of PCE.

4. Summary and Conclusions

We used the transparent replica fracture to carry out the visualization experiment of DNAPL residual and dissolution experiment. Through the software analysis of the photos, we studied the distribution characteristics of DNAPL in the migration process and the changes in the residual distribution in the dissolution process. The main conclusions are as follows:

(1) The migration front of DNAPL in the fracture was finger shaped, similar to that in porous media. The residual DNAPL droplets in the fracture were mainly concentrated in the range of 0.3 mm to 0.8 mm

(2) There was a good linear relationship between the concentration c of DNAPL and the area S, $c = 1.27S + 63.40$ ($R^2 = 0.97$). It was a simple and reliable method to use the area of DNAPL to replace the total amount when analyzing the experiment results

(3) The dissolution of DNAPL in the fractures was a process in which the dissolution rate changed from fast to slow. And there was an obvious tailing period. The dissolution rate of DNAPL increased significantly with the increase of the flow rate of water phase. In the dissolution process, the quantity of DNAPL hydrolysis reaction part accounted for 0.86% of the total residue on average, which could be ignored

However, there are some deficiencies in this study. This study only considered DNAPL phase and water phase and did not consider the influence of gas phase, which was different from the actual situation. Besides, this test only studied the residue and dissolution in a single fracture and did not extend to the complex fracture network. Therefore, there is still much work to be done.

Nomenclature

c: The concentration of PCE
Q: The displacement flow
Re: The Reynolds number
S: The variation of PCE's area
W: Aperture value
x: The chloride ion concentration
y: The light absorption value.

Greek Letters

ρ: The displacement fluid density
μ: The dynamic viscosity.

Data Availability

The data that support the findings of this study are available from the corresponding author (VS) upon reasonable request.

Conflicts of Interest

The authors declare that there are no conflicts of interest regarding the publication of this paper.

Acknowledgments

This research was supported by the National Natural Science Foundation of China (grant numbers 42177079 and 51709184) and the Central Public-Interest Scientific Institution Basal Research Fund (grant number Y122001).

References

[1] X. S. Yan, J. Z. Qian, L. Ma, M. Wang, and A. O. Hu, "Non-Fickian solute transport in a single fracture of marble parallel plate," *Geofluids*, vol. 2018, Article ID 7418140, 9 pages, 2018.

[2] C. Apollaro, I. Fuoco, A. Criscuoli, and A. Figoli, "Inorganic pollutants into groundwater: from geochemistry to treatment," *Geofluids*, vol. 2022, Article ID 9846802, 3 pages, 2022.

[3] S. Huling and J. Weaver, "Ground water issue: dense nonaqueous phase liquids," US Environmental Protection Agency, 1991.

[4] J. I. Gerhard, T. Pang, and B. H. Kueper, "Time scales of DNAPL migration in sandy aquifers examined via numerical simulation," *Ground Water*, vol. 45, no. 2, pp. 147–157, 2007.

[5] Y. B. Gao and J. D. Liu, "Effects of nonaqueous phase liquids pollution on the permeability and microstructure of in-filed and laboratory soaked contaminated clay soils," *Geofluids*, vol. 2022, Article ID 2767350, 17 pages, 2022.

[6] H. I. Essaid, B. A. Bekins, and I. M. Cozzarelli, "Organic contaminant transport and fate in the subsurface: evolution of knowledge and understanding," *Water Resources Research*, vol. 51, no. 7, pp. 4861–4902, 2015.

[7] A. Luciano, P. Viotti, and M. P. Papini, "Laboratory investigation of DNAPL migration in porous media," *Journal of Hazardous Materials*, vol. 176, no. 1-3, pp. 1006–1017, 2010.

[8] B. E. Sleep, S. Beranger, S. Reinecke, and Y. Filion, "DNAPL accumulation in wells and DNAPL recovery from wells: model development and application to a laboratory study," *Advances in Water Resources*, vol. 85, pp. 109–119, 2015.

[9] S. A. Bradford, K. M. Rathfelder, J. Lang, and L. M. Abriola, "Entrapment and dissolution of DNAPLs in heterogeneous porous media," *Journal of Contaminant Hydrology*, vol. 67, no. 1-4, pp. 133–157, 2003.

[10] C. Hofstee, M. Oostrom, J. H. Dane, and R. C. Walker, "Infiltration and redistribution of perchloroethylene in partially saturated, stratified porous media," *Journal of Contaminant Hydrology*, vol. 34, no. 4, pp. 293–313, 1998.

[11] B. H. Kueper and D. B. McWhorter, "The behavior of dense, the behavior of dense, nonaqueous phase liquids in fractured clay and rock," *Ground Water*, vol. 29, no. 5, pp. 716–728, 1991.

[12] B. H. Kueper and E. O. Frind, "An overview of immiscible fingering in porous media," *Journal of Contaminant Hydrology*, vol. 2, no. 2, pp. 95–110, 1988.

[13] Z. F. Zhang and J. E. Smith, "Visualization of DNAPL fingering processes and mechanisms in water-saturated porous media," *Transport in Porous Media*, vol. 48, no. 1, pp. 41–59, 2002.

[14] Y. W. Gao, F. Zhen, X. Q. Shi, Y. Y. Sun, H. X. Xu, and J. C. Wu, "Laboratory investigation of DNAPL migration behavior and distribution at varying flow velocities based on light transmission method," *Environmental Science*, vol. 36, no. 7, pp. 2532–2539, 2015.

[15] I. Dennis, J. Pretorius, and G. Steyl, "Effect of fracture zone on DNAPL transport and dispersion: a numerical approach," *Environment and Earth Science*, vol. 61, no. 7, pp. 1531–1540, 2010.

[16] R. Putzlocher, B. H. Kueper, and D. A. Reynolds, "Relative velocities of DNAPL and aqueous phase plume migration," *Journal of Contaminant Hydrology*, vol. 88, no. 3-4, pp. 321–336, 2006.

[17] M. Dejam, H. Hassanzadeh, and Z. X. Chen, "Shear dispersion in a fracture with porous walls," *Advances in Water Resources*, vol. 74, pp. 14–25, 2014.

[18] L. M. Abriola and G. F. Pinder, "A multiphase approach to the modeling of porous media contamination by organic compounds: 2. Numerical simulation," *Water Resources Research*, vol. 21, no. 1, pp. 19–26, 1985.

[19] K. Erning, S. Grandel, A. Dahmke, and D. Schäfer, "Simulation of DNAPL infiltration and spreading behaviour in the saturated zone at varying flow velocities and alternating subsurface geometries," *Environment and Earth Science*, vol. 65, no. 4, pp. 1119–1131, 2012.

[20] X. S. Chen, R. Hu, W. Guo, and Y. F. Chen, "Experimental observation of two distinct finger regimes during miscible displacement in fracture," *Transport in Porous Media*, vol. 144, no. 1, pp. 175–188, 2022.

[21] K. E. Christensen, P. W. Altman, C. Schaefer, and J. E. McCray, "Steady state DNAPL dissolution in three-dimensional fractured sandstone network experiments," *Journal of Environmental Engineering*, vol. 141, no. 1, article 04014047, 2015.

[22] W. Weerakone and R. Wong, "Affect of fracture characteristics on DNAPL-water flow in rock fractures," in *ISRM International Symposium on Rock Mechanics - SINOROCK 2009*, The University of Hong Kong, China, 2009.

[23] S. Zhu, J. H. Zheng, Z. D. Zhu, Q. Zhu, and L. Zhou, "Experiments on three-dimensional flaw dynamic evolution of transparent rock- like material under osmotic pressure," *Tunnelling and Underground Space Technology*, vol. 128, article 104624, 2022.

[24] B. Lu, J. R. Shao, and Y. Zhang, "Physical displacement and flush of entrapped LNAPL in fractured media groundwater," *China Environmental Science*, vol. 40, no. 1, pp. 182–189, 2020.

[25] Y. F. Chen, D. S. Wu, S. Fang, and R. Hu, "Experimental study on two-phase flow in rough fracture: phase diagram and localized flow channel," *International Journal of Heat and Mass Transfer*, vol. 122, pp. 1298–1307, 2018.

[26] J. Wan, T. K. Tokunaga, T. R. Orr, J. O'Neill, and R. W. Connors, "Glass casts of rock fracture surfaces: a new tool for studying flow and transport," *Water Resources Research*, vol. 36, no. 1, pp. 355–360, 2000.

[27] D. J. Brush and N. R. Thomson, "Fluid flow in synthetic rough-walled fractures: Navier-Stokes, Stokes, and local cubic law simulations," *Water Resources Research*, vol. 39, no. 4, p. 1085, 2003.

[28] S. E. Powers, I. M. Nambi, and G. W. Curry, "Non-aqueous phase liquid dissolution in heterogeneous systems: mechanisms and a local equilibrium modeling approach," *Water Resources Research*, vol. 34, no. 12, pp. 3293–3302, 1998.

[29] I. M. Nambi and S. E. Powers, "NAPL dissolution in heterogeneous systems: an experimental investigation in a simple heterogeneous system," *Journal of Contaminant Hydrology*, vol. 44, no. 2, pp. 161–184, 2000.

[30] S. Saenton and T. H. Illangasekare, "Upscaling of mass transfer rate coefficient for the numerical simulation of dense non-aqueous phase liquid dissolution in heterogeneous aquifers: upscaling of DNAPL dissolution," *Water Resources Research*, vol. 43, no. 2, article W02428, 2007.

[31] J. Zhu, J. F. Sykes, and J. F. Sykes, "Stochastic simulations of NAPL mass transport in variably saturated heterogeneous porous media," *Transport in Porous Media*, vol. 39, no. 3, pp. 289–314, 2000.